ACS Sustainable Chemistry & Engineering

Research Article

pubs.acs.org/journal/ascecg

Facile Fabrication of Flowerlike Natural Nanotube/Layered Double Hydroxide Composites as Effective Carrier for Lysozyme Immobilization

Yuanming Wang,[†,§] Chuochuo Liu,[†,§] Yatao Zhang,*[,†,‡] Bing Zhang,[†] and Jindun Liu*[,†]

[†]School of Chemical Engineering and Energy, Zhengzhou University, Zhengzhou 450001, China

[‡]School of Chemical Engineering, University of New South Wales, Sydney, New South Wales 2052, Australia

ABSTRACT: Carrier-based immobilization has been developed to enhance enzymatic stability and activity, which permits the employment of enzymes in different solvents, at wide ranges of pH and temperature as well as high substrate concentrations. In this study, a novel carrier was prepared with halloysite nanotubes (HNTs) and layered double hydroxide (LDH) via a layer-by-layer (LbL) deposition process followed by an in situ growth technique. The in situ growth of LDH nanoplatelets on a HNTs support was demonstrated producing a well-defined three-dimensional architecture (HNTs@LDH). These flowerlike structural materials possess a high lysozyme immobilized amount (237.6 mg/g support) compared with individual HNTs and LDH. And such lysozyme immobilized composites (HNT@LDH−Ly) exhibit a superior antibacterial property against *Escherichia coli* (*E. coli*).

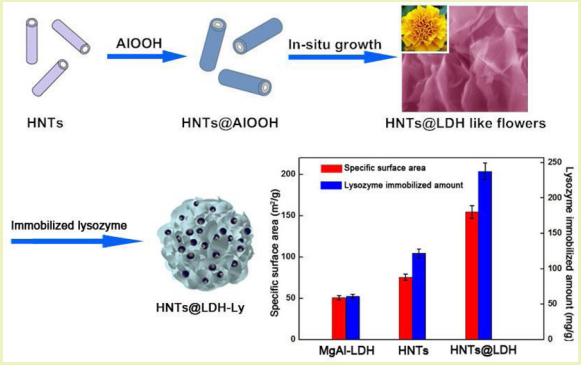

KEYWORDS: *Layered double hydroxide, Halloysite nanotubes, In situ growth, Enzyme immobilization*

INTRODUCTION

The anchoring of an enzyme onto a functional support has been developed, which can address lots of issues of free enzymes, such as instability, low activity, difficulty to retain and sensitivity toward their environment.[1−7] It is generally acknowledged that an ideal enzyme host primarily has a huge surface area and modifiable surface, as well as chemical and mechanical stability.[2] In recent years, much effort has been made in obtaining satisfying support. For instance, graphene oxide (GO) nanosheets have been employed as a matrix to study enzyme immobilization.[8] Most recently, some antibacterial materials based on an immobilized enzyme, such as lysozyme-layered double hydroxide nanocomposites[9] and enzyme-functionalized porous zirconia microtubes,[10] have been developed and show effective antibacterial performance.

Halloysite nanotubes (HNTs), one predominant form with a hollow tubular structure in the submicrometer range, were found to be a viable and inexpensive nanoscale container for the encapsulation of biologically active molecules.[11−15] Two-dimensional inorganic solids, such as layered double hydroxide (LDH), also defined as anionic clays, are considered more biocompatible and nontoxic than other inorganics, which makes them very appropriate for the immobilization of anions and biomolecules.[16−19] The above reports on the immobilization of enzymes with HNTs or LDH demonstrated the production of retentively active, catalytic and recyclable materials. However, the amount and activity of enzymes immobilized on HNTs or LDH by the adsorption method is very low, which has a direct effect on the catalytic efficiency of the unit mass of a biocomposite. The reason is that the specific surface area of support is small and HNTs could prevent enzyme[14] (negatively charged during immobilization process) adsorption on its negatively charged outer surface. Therefore, a novel three-dimensional architecture based on HNTs (one-dimension) and LDH (two-dimension) will be an effective route to obtain improved enzyme support.

To our knowledge, there are no reports on the three-dimensional architecture consisting of HNTs and LDH. Herein, we report a facile and efficient synthesis of HNTs@LDH composites via a layer-by-layer (LbL) deposition process followed by an in situ growth technique[20] and the subsequent enzyme immobilization is carried out by an adsorption method. Our strategy (Figure 1) is based on the LbL deposition of AlOOH primer on HNTs, and then an in situ crystallization of MgAl−LDH nanoplatelets on the surface of HNTs@AlOOH nanotubes is carried out. The resulting HNTs@LDH composites display a three-dimensional flowerlike morphology with superior properties, and then are used for the immobilization of lysozyme (an antimicrobial protein that has an isoelectric point without specific ionic adsorption at 11.3).[21] Moreover, the amount of lysozyme immobilization on the surface of HNTs@LDH composites is enhanced greatly,

Received: February 10, 2015
Revised: April 19, 2015
Published: April 28, 2015

DOI: 10.1021/acssuschemeng.5b00104
ACS Sustainable Chem. Eng. 2015, 3, 1183−1189

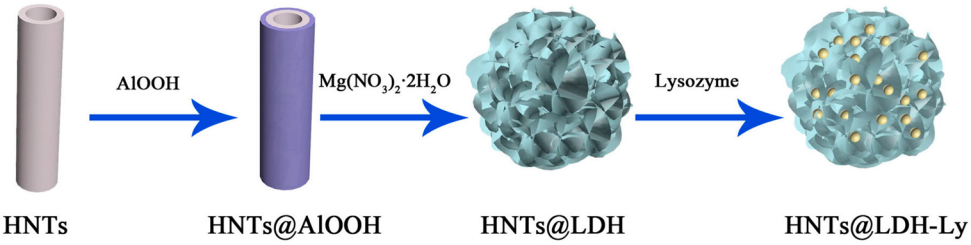

Figure 1. Schematic representations of the overall preparation process of HNTs@LDH. Yellow spheres indicate lysozyme molecules.

compared with that of individual HNTs and LDH that was synthesized by our previous method.[22] This facile method for generation of HNTs@LDH-based flowerlike structure will promote the utilization of structured materials with excellent selective adsorption in various potential fields.

According to a previously published method,[23] boehmite nanoparticles with sizes of 15−30 nm were synthesized on addition of NaOH to a solution of $Al(NO_3)_3·9H_2O$ as the source of aluminum. Then HNO_3 was slowly added dropwise into aqueous solution of AlOOH to obtain a collosol. Next, HNTs were dispersed in the above solution under vigorous stirring and a subsequent LbL deposition process resulted in a continuous and uniform AlOOH coating formation on the surface of the HNTs. And the coated nanotubes were obtained after washing, centrifugation and drying. The whole process (dispersion, withdrawing, drying) was repeated multiple times until the supernate contained no white AlOOH by centrifugation. It is worth mentioning that the AlOOH coating plays a key role in the growth of ordered LDH nanocrystals. A nanoplatelet of MgAl−LDH was formed by reaction of the AlOOH coating deposited on the surface of HNTs with a mixing aqueous solution of $Mg(NO_3)_2·6H_2O$ and urea at 80 °C. Subsequently, the mixture was slowly cooled to room temperature and the material HNTs@MgAl−LDH was isolated by centrifugation, rinsing repeatedly with ethanol and drying at room temperature. Finally, in a typical experiment, HNTs@MgAl−LDH was added into Lysozyme phosphate buffer solution and the mixture was incubated for 4 h under the condition of shaking for the immobilization of lysozyme. After centrifugation, the immobilized enzyme was rinsed several times in the same phosphate buffer to remove physical adsorbed enzyme. Then the resulting composites were dried and stored at 4 °C. For comparison, the adsorption capacity of MgAl−LDH and HNTs toward lysozyme was investigated under identical conditions.

EXPERIMENTAL SECTION

Materials. Halloysite nanotubes (HNTs) were refined from clay minerals in Henan province, China. The test strains, *Escherichia coli* (8099), used for this study were provided by College of Public Health of Zhengzhou University. Lysozyme and fluorescein isothiocyanate were obtained from J&K Scientific Co. Ltd., China, and were used without further purification. All other regents were of analytical reagent grade. The water used was deionized water.

Synthesis of AlOOH. The boehmite nanoparticles were prepared based on a previously published method. In a typical synthesis, NaOH (6.49 g) and $Al(NO_3)_3·9H_2O$ (20 g) were respectively dispersed in 50 and 30 mL of deionized water under the conditions of ultrasonication. Then the NaOH solution was slowly added (3 mL per minute) to the $Al(NO_3)_3·9H_2O$ solution with vigorous stirring at room temperature. When the addition was complete, the resulting milky mixture was subjected to an ultrasonic bath for 3 h. Subsequently, the products were filtered and washed repeatedly with distilled water, followed by drying in the oven at 220 °C for 4 h.

Synthesis of HNTs@AlOOH. 5.8 g of solid boehmite was dispersed in 107 mL of deionized water, and solution was stirred for 1 h at 85 °C. HNO_3 (9.5 mL, 1.0 M) was then added dropwise, and the mixture was refluxed gently with stirring for a further period of 6 h. After cooling to room temperature, the AlOOH primer sol was obtained. Next, HNTs were dispersed in AlOOH primer sol with vigorous stirring for 1 h. The products were withdrawn by precipitating and washing repeatedly with ethanol, followed by drying in air for 30 min. The whole process (dispersion, withdrawing, drying) was repeated multiple times until the supernate contained no white AlOOH by centrifugation. The resulting material, HNTs@AlOOH, was dried in a vacuum at 35 °C for 24 h.

Synthesis of HNTs@LDH. 0.3 g of HNTs@AlOOH was added to a solution containing 0.005 mol $Mg(NO_3)_2·6H_2O$, 0.04 mol urea and 200 mL of deionized water. Subsequently, the mixture was heated to 80 °C and continually stirred for 24 h, and then it was slowly cooled to room temperature. Finally, HNTs@MgAl−LDH was isolated by centrifuging and rinsing repeatedly with ethanol, and dried at room temperature.

Synthesis of HNTs@LDH Sample Loading with Lysozyme. The enzyme stock solution was prepared by dissolving lysozyme in phosphate buffer (0.2 M Na_2HPO_4, 0.2 M NaH_2PO_4, pH 6.2). In a typical experiment, 0.1 g of HNTs@MgAl−LDH was added into lysozyme solution (1.5 mg/mL). The mixture was incubated for 4 h under the condition of shaking at 15 °C and then centrifuged at 8000 rpm for 8 min. After that, the supernatant was collected to determine the amount of loading enzyme. The immobilized enzymes were rinsed three times with the same buffer to remove physical adsorbed enzyme. The resulting material was dried and stored at 4 °C. For comparison, MgAl−LDH and HNTs loadings with lysozyme were prepared under the same conditions (temperature, shaking speed and shaking time) in phosphate buffer (pH 6.2).

Characterization. X-ray diffraction (XRD) was carried out on a PAN Alytical X'Pert Pro by use of copper Kα as the source of radiation, with a scan step of 0.02° and a scan range between 5° and 50°. The morphology, dimension and elemental analyses of the samples were inspected by use of a JEOL Model JSM-6700F scanning electron microscope (Tokyo, Japan) equipped with energy dispersive X-ray (EDX) spectrometry (EDS). An FEI model TECNAI G^2 transmission electron microscope (FEI, America) was used for the determination of HNTs−LDH. The surface areas of samples were measured with a surface area apparatus (BET method). The immobilization and distribution of lysozyme on the surface of HNTs−LDH were examined by a BM-21AY fluorescence microscope (Shanghai BM optical instrument manufacturing co., Ltd., China) with the excitation wavelength of 450−490 nm.

Minimum Inhibitory Concentration (MIC). First, the target *E. coli* bacteria were cultured to a mid log phase in Luria−Bertani (LB) broth at 37 °C and 10^6 CFU/mL *E. coli* cells suspension was prepared for the following utilization. Serial dilutions of the antibacterial agent (512, 256, 128, 64, 32 μg/mL) were performed in LB that was inoculated with 5×10^5 CFU/mL of bacteria at 37 °C for 2 h. 100 μL of the above bacterial suspension, after being diluted 10^4 times, was cultured on an agar plate. Growth of the cells was determined by observing the turbidity of the culture. The lowest concentration, at which no visual

DOI: 10.1021/acssuschemeng.5b00104
ACS Sustainable Chem. Eng. 2015, 3, 1183−1189

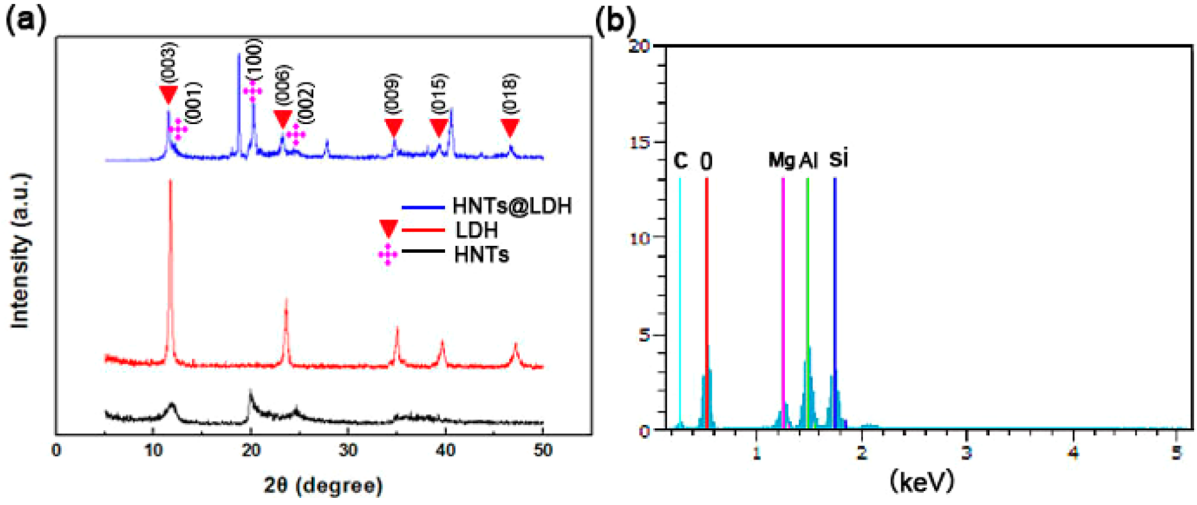

Figure 2. (a) XRD patterns of HNTs, LDH and HNTs@LDH; (b) EDS spectra of HNTs@LDH.

turbidity could be observed, represented the MIC of the antibacterial material.

Bacteriostasis Rate. 100 mL of the above-mentioned bacterial suspension, after being diluted 10^5 times, was cultured on an agar plate. After incubation at 37 °C for 16 h, the colonies were counted and the bacteriostasis rate was determined by dividing the number of colony-forming units (CFU) that are killed by antibacterial reagent by the number of CFU of the control group.

RESULTS AND DISCUSSION

Figure 2a shows the XRD patterns of HNTs, LDH and HNTs@LDH. The diffraction peaks that HNTs and LDH show are in good agreement with the characteristic peaks of the standard compound Halloysite-7 Å (JCPDS Card No. 29-1487) and $Mg_{0.667}Al_{0.33}(OH)_2(CO_3)_{0.167}(H_2O)_{0.5}$ (JCPDS Card No. 89-0460). After the in situ growth process, the XRD pattern of the resulting HNTs@LDH composites exhibits superimposition of reflections of a HNTs phase and a LDH phase. The diffraction peaks for the (003), (006), (009), (015) and (018) crystal planes are clearly observed, indicating the well-formed crystalline layered structure. In addition, the elemental analysis of the as-prepared HNTs@LDH was recorded by EDS, shown in Figure 2b. Typical elements on the HNTs (O, Si, Al) and LDH (Mg, Al, C) were observed in the EDS spectrum, demonstrating the successful growth of LDH crystallization on the modified HNTs.

To investigate the growth process for construction of the flowerlike structure of HNTs@LDH composites, typical field emission scanning electron microscopy (FE-SEM) and transmission electron microscopy (TEM) studies were employed. As is shown in the TEM image (Figure 3a), HNTs, consisting of a two-layered aluminosilicate, have a submicrometer sized hollow cylindrical morphology. The size of halloysite tubules is 600 ± 200 nm in length, 30 nm in external diameter and 15 nm in lumen. And halloysite particles have good dispersibility and colloidal stability in water due to negative electrical ζ-potential in a wide range of pH. The morphology of HNTs@LDH composites was investigated by use of high resolution scanning electron microscopy. The SEM images (Figure 3c,d) clearly demonstrated that lots of flowerlike architectures with a high crystallinity quality were synthesized and these particles were totally well-dispersed. In addition, as can be seen from the enlarged images (Figure 3e,f), the flowerlike architectures are composed of dense platelets with a microsized width and

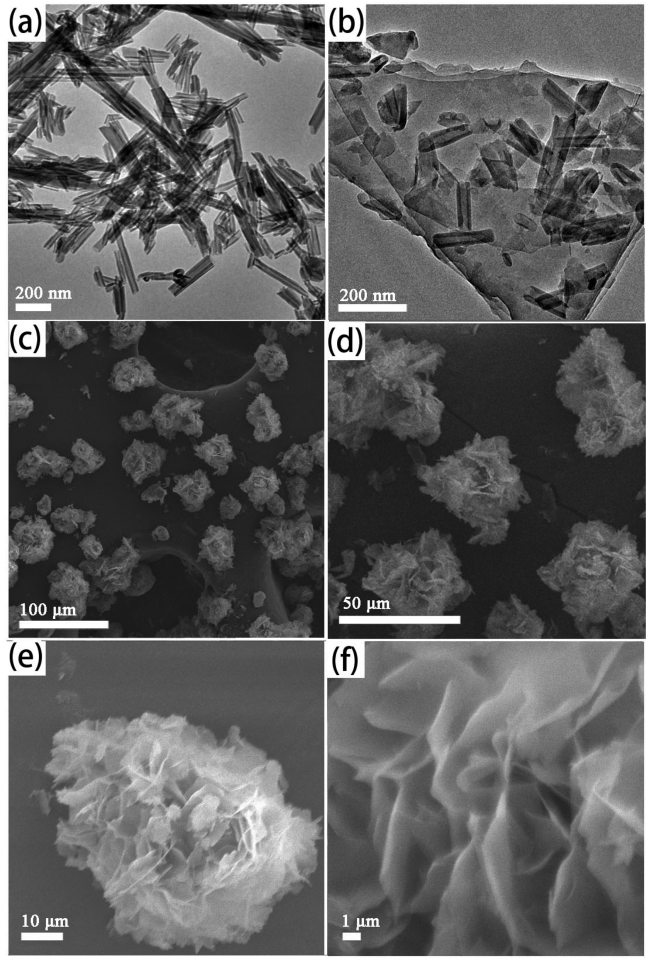

Figure 3. TEM images of raw HNTs (a) and HNTs@LDH nanosheets (b). Different magnification SEM images of HNTs@LDH (c, d, e and f).

length, and the thickness of these platelets are uniform (ca. 100 nm). To investigate the inherent structure of the platelets, transmission electron microscopy was used. The TEM image (Figure 3b) confirms random HNTs embedded within the platelet that looks like a sandwich structure as a result of in situ crystallization. Similarly, in previous work, Yu et al.,[24]

DOI: 10.1021/acssuschemeng.5b00104
ACS Sustainable Chem. Eng. 2015, 3, 1183−1189

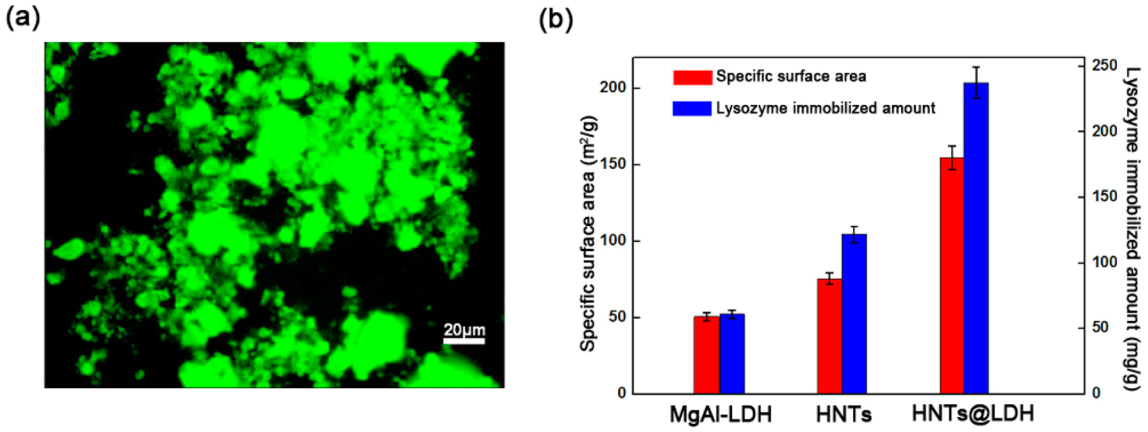

Figure 4. (a) Fluorescence microscopy image of FITC labeled lysozymes on HNTs@LDH surface; (b) specific surface area and lysozyme immobilized amount of different samples.

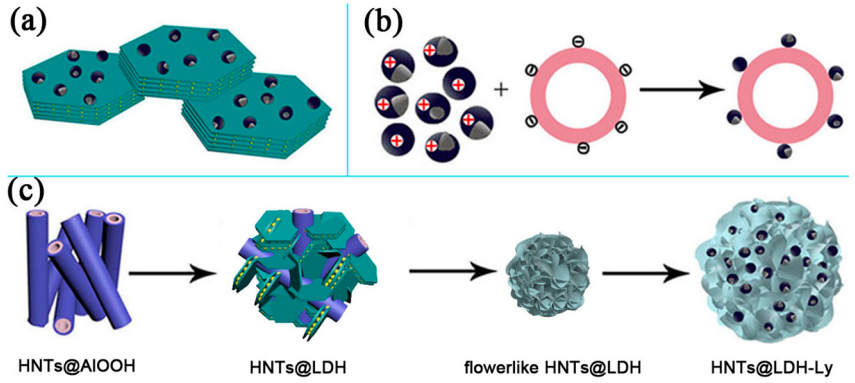

Figure 5. Scheme illustration showing (a) immobilization of lysozyme on LDH; (b) principle process of immobilization of lysozyme on HNTs; (c) proposed mechanism of formation of flowerlike structural HNTs@LDH composites, comprising three steps: (I) deposition of precursors on the support; (II) formation and growth of primary crystals; (III) formation of flowerlike structures. The last step shows the image of lysozyme immobilized by flowerlike structural HNTs@LDH.

introduced HNTs to graphene−AgNPs-based nanocomposites combining the adhesive ability of DOPA to fabricate a sandwich-like nanomaterial based on the interpenetrative nanocomposites. It is well-known that LDH crystallites with a hydrotalcite-like structure tend to have a platelet morphology in which the dimensions of the width are much larger than the thickness. Based on this, the typical nanosheets of LDH can be observed in the image (Figure 3b).

As is mentioned above, lysozyme has an isoelectric point without specific ionic adsorption at 11.3, suggesting that lysozyme is positive in a wide pH. However, given the fact that the nanosheets of LDH carry a positive charge, it is an unfavorable factor for the binding of lysozyme. As we know, protein adsorption is a complex process that depends on a number of factors in addition to electrostatic interaction. To observe whether lysozyme could be immobilized on HNTs@LDH composites, lysozyme was labeled with fluorescein isothiocyanate (FITC), and then the labeled lysozymes were used for the immobilization process. Next, the FITC-tagged HNTs@LDH composites were observed by a fluorescence microscope. From the fluorescent image (Figure 4a), the products combining FITC-tagged lysozymes and HNTs@LDH composites display a bright green color, suggestive of the successful immobilization of lysozyme on the surface of HNTs@LDH composites. The result also indicates that electrostatic interaction is not the key factor in determining the adsorption behavior of HNTs@LDH composites. Currently, the proposed mechanisms of LDH for the protein adsorption mainly include electrostatic attraction, ion exchange, van der Waals interaction and hydrogen bonding. For efficient immobilization via van der Waals interaction, both the carrier and the enzyme need to have large lipophilic surface areas. However, the LDH is very hydrophilic, which is unfavorable for the van der Waals interaction. And lysozyme is positive in the immobilization process and it can not perform anion exchange. So, the hydrogen bonding should be the main factor in determining the adsorption behavior of HNTs@LDH composites.

Currently, materials of loading enzyme have been widely used in the field of catalysis, but the amount of enzyme immobilization has a significant effect on catalytic hydrolysis of the materials of loading lysozyme. In this work, we investigate the amount of lysozyme immobilized on HNTs@LDH composites. As a control experiment, lysozyme was reacted with LDH and HNTs under identical conditions. And the amount of lysozyme immobilization, specific surface areas of LDH, HNTs and HNTs@LDH were calculated, and the value is presented in Figure 4b. As can be seen clearly, the HNTs@LDH exhibits a binding capacity for lysozyme of 237.6 mg/g and has a huge specific surface area of 154.6 m^2/g, much larger than those of native LDH (61.0 mg/g, 50.7 m^2/g) and HNTs

DOI: 10.1021/acssuschemeng.5b00104
ACS Sustainable Chem. Eng. 2015, 3, 1183−1189

(121.8 mg/g, 75.6 m^2/g). This demonstrates that the adsorption capacity of HNTs@LDH is improved greatly.

To illustrate the immobilization mechanism better, a proposed schematic illustration is shown in Figure 5. For LDH (Figure 5a), the nanosheets stack alternately with appropriately counter-charged nanosheets according to a coprecipitation reaction as previously reported.[25] However, the self-stack effect makes LDH flakes possess less specific surface area than that of single LDH nanosheets. Thus, lysozymes only bind to the exposed outer surface and meanwhile, the positively charged surface of LDH prevents lysozyme adsorption. The explanation is in good agreement with the low lysozyme immobilized amount of LDH. The ζ-potential behavior of HNTs (Figure 5b) is mostly negative in the pH range 6−7 due to the surface potential of SiO_2 with a small contribution from the positive Al_2O_3 inner surface.[26] Therefore, lysozyme that remained positively charged during the immobilization process was immobilized on the negatively charged outer surface through ionic adsorption binding. In the third illustration (Figure 5c), the proposed mechanism for the formation of flowerlike structure contains mainly three steps. At an early stage (step 1), deposition of precursors (AlOOH) is carried out on the support via a LbL deposition process. At this stage, HNTs form composites (HNTs@AlOOH) with AlOOH, predominantly attributed to the existence of abundant hydroxyl groups of the outermost surface of HNTs. These composites provide a location for nucleation of the primary crystals. And it has been confirmed that the AlOOH coating plays a key role in providing the necessary aluminum source for the growth of ordered LDH nanocrystals.[20] At the second stage (step 2), the AlOOH coating deposited on the surface of HNTs reacts with the mixing aqueous solution of Mg $(NO_3)_2 \cdot 6H_2O$ and urea, resulting in the formation of LDH crystalline nuclei on HNTs. As the reaction continues, these crystalline nuclei gradually grow to form many scraggly interlaced 2D thin nanosheets. At the third stage (step 3), as we know lots of HNTs often aggregate together, each of them will perform the growth of LDH nanosheets. And the thin nanosheets anisotropic growth on the aggregation of HNTs will results in preliminary formation of a branched flowerlike structure. In the proposed growth process, HNTs act as the backbone to bind the petals together. And the mechanism is that it tends to form single LDH nanosheets under the condition of the existence of support matrix, which makes HNTs@LDH own a much larger specific surface area (154.6 m^2/g) than that of LDH (50.7 m^2/g) and HNT (75.6 m^2/g). The high amount of lysozyme immobilization (237.6 mg/g) of HNTs@LDH can be attributed to the huge specific surface area that provides abundant docking sites for enzymes.

To evaluate the adsorption property of HNTs@LDH, a comparison about the amount of enzyme immobilization was made with several reported immobilization materials which immobilize enzymes via a simple adsorption method. And the relation between the dimension of immobilization materials and the amount of enzyme immobilization is shown in Figure 6. Clearly, the immobilized amount of 3D architectural materials is highest compared with that of other dimensional materials. Moreover, it was found that the enzyme immobilized amount of two 3D architectural materials was very close, indicating that our composites can match with the flowerlike Fe_3O_4@SiO_2@NiAlLDH microspheres. Thus, although several types of ordered LDH structures have been developed, the fabrication of LDH with a well-defined 3D structure is supposed to be an alternative strategy to enhance their application in adsorption as well as separation of biological molecules.

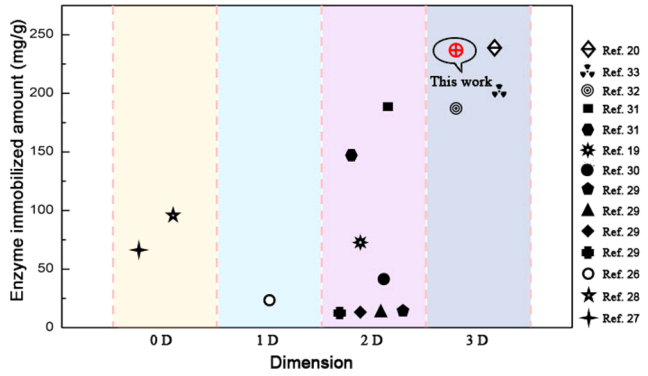

Figure 6. Comparison of enzyme immobilized amount among several materials with different morphologies[19,20,26−33]

Enzymatic activity is a significant parameter to estimate the properties of immobilized enzyme. Then the immobilized lysozyme (HNTs@LDH−Ly) was applied in an antibacterial test. Subsequently, minimum inhibitory concentration (MIC), defined as the lowest concentration of an antimicrobial that will inhibit the visible growth of a microorganism after overnight incubation, was obtained to evaluate the antibacterial capacity of the HNTs@LDH−Ly. The test results are presented in Figure 7. Apparently, from the pictures, it can be seen that the agar plate containing the culture solution of HNTs@LDH−Ly presents less bacterial colonies than that of the control group. This is because of the hydrolysis of immobilized lysozyme toward the cell wall of *E. coli* bacteria. And the obtained MIC and bacteriostasis rate are 256 μg/mL and 96.2% respectively, indicating a good antibacterial capacity of HNTs@LDH−Ly composites. Moreover, from the comparison of MIC of immobilized lysozyme and free lysozyme (MIC, 1.25 mg/mL), the antibacterial activity of immobilized lysozyme improves nearly five times, which makes it a promising antibacterial material.

To illustrate whether the HNTs@LDH was an appropriate carrier for the immobilization of lysozyme, an activity comparison of recent lysozyme immobilization materials was made with HNTs@LDH−Ly. For example, Sun et al.[34] functionalized carbon nanotubes with an ionic surfactant (sodium hexadecyl sulfate, SHS) and the functionalized CNTs were utilized to adsorb lysozyme. The results showed that the conjugate of lysozyme−SHS−CNT retained 83% activity of the free lysozyme. This activity was much higher than that of the lysozyme−CNT, which retained 55% activity of the free lysozyme. Kao et al.,[35] studied specifically the protein immobilized in the nanochannels and it was found that the activity of the lysozyme immobilized in the 5.6 nm mesopores of MSNs was higher than that of native enzymes (~2.5 times). Han et al.[36] detractively interacted positive lysozyme with negative titanate nanosheets to form a bioinorganic composite and after immobilization, the enzyme showed the activity retention (26%). Yang et al.[9] prepared lysozyme-layered double hydroxide nanocomposites (LYZ−LDHs) by intercalating LYZ in LDH for the first time. At pH 7, the activities of unit mass LYZ in LYZ1.6−LDH, LYZ0.8−LDH and LYZ0.4−LDH were 57.9%, 74.0% and 97.5% per unit mass of free LYZ, respectively, showing that immobilized LYZ generally have lower enzyme activity than free LYZ. By comparison, it was found that lysozyme immobilized on HNTs@LDH had higher

DOI: 10.1021/acssuschemeng.5b00104
ACS Sustainable Chem. Eng. 2015, 3, 1183−1189

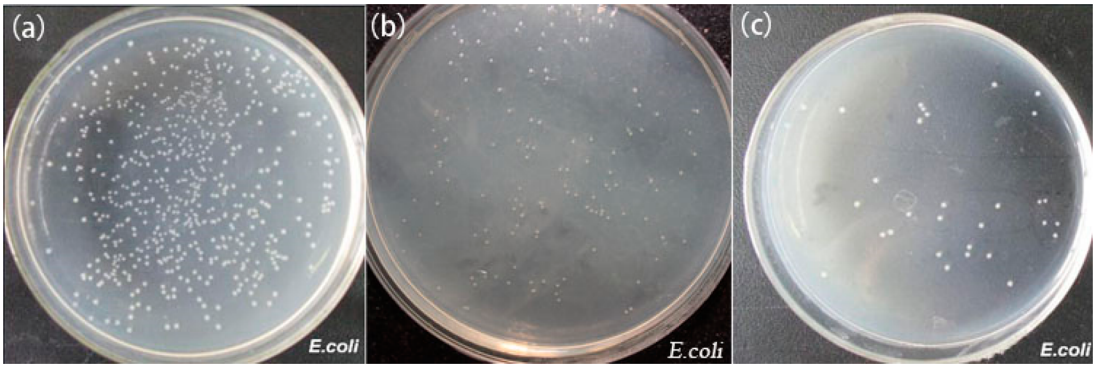

Figure 7. Photographs showing bacterial colonies of the culture on agar plates inoculated with *E. coli* cells suspension (a) *E. coli* cells suspension containing 256 μg/mL of lysozyme (b) and 256 μg/mL of HNTs@LDH−Ly (c).

activity than that of the materials mentioned above and demonstrated that it was an appropriate carrier for the immobilization of lysozyme.

It is well-known that the antibacterial activity of lysozyme is considered to be strongly related to its spatial structure. It has already been found experimentally that the lysozyme molecule structure is not changed much when it is adsorbed on a flat, charged surface.[37] So, lysozyme may exhibit the same or even higher activity than in solution. As we know, both of the nanosheets of LDH and lysozyme carry a positive charge. Combination of them will form a stronger electrostatic field and produce a multivalent interaction.[38] The multivalent interaction will lead to high binding affinity and significantly increase the adhesive interaction between HNTs@LDH−Ly and *E. coli* (Gram-negative) and make it easier for lysozyme to lyse the bacteria adsorbed on the HNTs@LDH−Ly composites, producing higher activity than that of free lysozyme.

In summary, we have demonstrated a novel HNTs@LDH-based flowerlike structure that is constructed by in situ growth of LDH nanoplatelets on the surface of HNTs. The prepared HNTs@LDH exhibits well-defined three-dimensional architecture and large surface area that renders it ideal candidates as host for biomolecules. The immobilized amount for lysozyme is up to 237.6 mg/g support because the HNTs@LDH platelets provide abundant docking sites for lysozyme. Moreover, the improved activity of lysozyme makes it a promising antibacterial material. A practical application of HNTs@LDH−Ly was successfully demonstrated in *E. coli* bacteria and it exhibited excellent antibacterial effect. Therefore, this work provides a facile and efficient approach for the fabrication of a HNTs@LDH flowerlike structure that has potential applications in a variety of biomedical fields including protein separation and purification, drug delivery, and the composites of HNTs@LDH and enzyme can be further applied in antibiosis, catalysis and other fields.

AUTHOR INFORMATION

Corresponding Authors

*Y. Zhang. Tel.: +86-371-67781734. Fax: +86-371-67739348. E-mail: zhangyatao@zzu.edu.cn.

*J. Liu. E-mail: liujindun@zzu.edu.cn.

Author Contributions

§These authors contributed equally.

Notes

The authors declare no competing financial interest.

ACKNOWLEDGMENTS

This work was financially sponsored by the National Natural Science Foundation of China (Nos. 21376225 and 21476215), and Excellent Youth Development Foundation of Zhengzhou University (No. 1421324066). We sincerely acknowledge the financial assistance of visiting research program in University of New South Wales by the China Scholarship Council (No. 201208410135).

REFERENCES

(1) Seleci, M.; Ag, D.; Yalcinkaya, E. E.; Demirkol, D. O.; Guler, C.; Timur, S. Amine-intercalated montmorillonite matrices for enzyme immobilization and biosensing applications. *RSC Adv.* **2012**, *2* (5), 2112−2118.

(2) Hanefeld, U.; Gardossi, L.; Magner, E. Understanding enzyme immobilisation. *Chem. Soc. Rev.* **2009**, *38* (2), 453−468.

(3) Brady, D.; Jordaan, J. Advances in enzyme immobilisation. *Biotechnol. Lett.* **2009**, *31* (11), 1639−1650.

(4) Zhang, Y.-T.; Dai, X.-G.; Xu, G.-H.; Zhang, L.; Zhang, H.-Q.; Liu, J.-D.; Chen, H.-L. Modeling of CO_2 mass transport across a hollow fiber membrane reactor filled with immobilized enzyme. *AIChE J.* **2012**, *58* (7), 2069−2077.

(5) Zhang, Y.-T.; Zhang, L.; Chen, H.-L.; Zhang, H.-M. Selective separation of low concentration CO_2 using hydrogel immobilized CA enzyme based hollow fiber membrane reactors. *Chem. Eng. Sci.* **2010**, *65* (10), 3199−3207.

(6) Zhang, Y.-T.; Fan, L.-H.; Zhi, T.-T.; Zhang, L.; Huang, H.; Chen, H.-L. Synthesis and characterization of poly(acrylic acid-co-acrylamide)/hydrotalcite nanocomposite hydrogels for carbonic anhydrase immobilization. *J. Polym. Sci., Polym. Chem.* **2009**, *47* (13), 3232−3240.

(7) Zhang, Y.-T.; Zhi, T.-T.; Zhang, L.; Huang, H.; Chen, H.-L. Immobilization of carbonic anhydrase by embedding and covalent coupling into nanocomposite hydrogel containing hydrotalcite. *Polymer* **2009**, *50* (24), 5693−5700.

(8) Zhang, J.; Zhang, F.; Yang, H.; Huang, X.; Liu, H.; Zhang, J.; Guo, S. Graphene oxide as a matrix for enzyme immobilization. *Langmuir* **2010**, *26* (9), 6083−6085.

(9) Yang, Q. Z.; Chang, Y. Y.; Zhao, H. Z. Preparation and antibacterial activity of lysozyme and layered double hydroxide nanocomposites. *Water Res.* **2013**, *47* (17), 6712−6718.

(10) Kroll, S.; Brandes, C.; Wehling, J.; Treccani, L.; Grathwohl, G.; Rezwan, K. Highly efficient enzyme-functionalized porous zirconia microtubes for bacteria filtration. *Environ. Sci. Technol.* **2012**, *46* (16), 8739−8747.

(11) Shchukin, D. G.; Sukhorukov, G. B.; Price, R. R.; Lvov, Y. M. Halloysite nanotubes as biomimetic nanoreactors. *Small* **2005**, *1* (5), 510−513.

(12) Lvov, Y. M.; Shchukin, D. G.; Mohwald, H.; Price, R. R. Halloysite clay nanotubes for controlled release of protective agents. *ACS Nano* **2008**, *2* (5), 814−820.

DOI: 10.1021/acssuschemeng.5b00104
ACS Sustainable Chem. Eng. 2015, 3, 1183−1189

(13) Liu, C.; Yu, L.; Zhang, Y.; Zhang, B.; Liu, J.; Zhang, H. Preparation of poly(sodium acrylate-acrylamide) superabsorbent nanocomposites incorporating graphene oxide and halloysite nanotubes. *RSC Adv.* **2013**, *3* (33), 13756−13763.
(14) Zhai, R.; Zhang, B.; Liu, L.; Xie, Y.; Zhang, H.; Liu, J. Immobilization of enzyme biocatalyst on natural halloysite nanotubes. *Catal. Commun.* **2010**, *12* (4), 259−263.
(15) Lvov, Y.; Abdullayev, E. Functional polymer-clay nanotube composites with sustained release of chemical agents. *Prog. Polym. Sci.* **2013**, *38* (10−11), 1690−1719.
(16) Zhang, Y.; Fan, L.; Cheng, L.; Zhang, L.; Chen, H. Preparation and morphology of high-performance exfoliated poly(sodium acrylate)/hydrotalcite nanocomposite superabsorbents. *Polym. Eng. Sci.* **2009**, *49* (2), 264−271.
(17) Zhang, Y.; Fan, L.; Zhao, P.; Zhang, L.; Chen, H. Preparation of nanocomposite superabsorbents based on hydrotalcite and poly(acrylic-co-acrylamide) by inverse suspension polymerization. *Compos. Interfaces* **2008**, *15* (7−9), 747−757.
(18) Zhang, Y.; Zhang, Y.; Zhang, H.; Liu, J. Preparation and flame resistance of hydrotalcite/epoxy nanocomposites containing red phosphorous. *Adv. Mater. Res.* **2011**, *194*−*196*, 1460−1463.
(19) Frey, S. T.; Guilmet, S. L.; Egan, R. G., 3rd; Bennett, A.; Soltau, S. R.; Holz, R. C. Immobilization of the aminopeptidase from *Aeromonas proteolytica* on Mg^{2+}/Al^{3+} layered double hydroxide particles. *ACS Appl. Mater. Interfaces* **2010**, *2* (10), 2828−2832.
(20) Shao, M.; Ning, F.; Zhao, J.; Wei, M.; Evans, D. G.; Duan, X. Preparation of Fe_3O_4@SiO_2@layered double hydroxide core-shell microspheres for magnetic separation of proteins. *J. Am. Chem. Soc.* **2012**, *134* (2), 1071−1077.
(21) Dismer, F.; Petzold, M.; Hubbuch, J. Effects of ionic strength and mobile phase pH on the binding orientation of lysozyme on different ion-exchange adsorbents. *J. Chromatogr. A* **2008**, *1194* (1), 11−21.
(22) Liu, J.; Yu, L.; Zhang, Y. Fabrication and characterization of positively charged hybrid ultrafiltration and nanofiltration membranes via the in-situ exfoliation of Mg/Al hydrotalcite. *Desalination* **2014**, *335* (1), 78−86.
(23) Rajabi, L.; Derakhshan, A. A. Room temperature synthesis of boehmite and crystallization of nanoparticles: Effect of concentration and ultrasound. *Sci. Adv. Mater.* **2010**, *2* (2), 163−172.
(24) Yu, L.; Zhang, Y.; Zhang, B.; Liu, J. Enhanced antibacterial activity of silver nanoparticles/halloysite nanotubes/graphene nanocomposites with sandwich-like structure. *Sci. Rep.* **2014**, *4*, 4551.
(25) Iyi, N.; Ebina, Y.; Sasaki, T. Water-swellable MgAl-LDH (layered double hydroxide) hybrids: Synthesis, characterization, and film preparation. *Langmuir* **2008**, *24* (10), 5591−5598.
(26) Zhai, R.; Zhang, B.; Wan, Y.; Li, C.; Wang, J.; Liu, J. Chitosan−halloysite hybrid-nanotubes: Horseradish peroxidase immobilization and applications in phenol removal. *Chem. Eng. J.* **2013**, *214*, 304−309.
(27) Liu, X.; Lei, L.; Li, Y.; Zhu, H.; Cui, Y.; Hu, H. Preparation of carriers based on magnetic nanoparticles grafted polymer and immobilization for lipase. *Biochem. Eng. J.* **2011**, *56* (3), 142−149.
(28) Vinoba, M.; Bhagiyalakshmi, M.; Jeong, S. K.; Yoon, Y. I.; Nam, S. C. Immobilization of carbonic anhydrase on spherical SBA-15 for hydration and sequestration of CO_2. *Colloids Surf., B* **2012**, *90*, 91−96.
(29) Safari Sinegani, A. A.; Emtiazi, G.; Shariatmadari, H. Sorption and immobilization of cellulase on silicate clay minerals. *J. Colloid Interface Sci.* **2005**, *290* (1), 39−44.
(30) Bayramoglu, G.; Senkal, B. F.; Arica, M. Y. Preparation of clay−poly(glycidyl methacrylate) composite support for immobilization of cellulase. *Appl. Clay Sci.* **2013**, *85*, 88−95.
(31) Tzialla, A. A.; Pavlidis, I. V.; Felicissimo, M. P.; Rudolf, P.; Gournis, D.; Stamatis, H. Lipase immobilization on smectite nanoclays: Characterization and application to the epoxidation of alpha-pinene. *Bioresour. Technol.* **2010**, *101* (6), 1587−1594.
(32) Na, W.; Wei, Q.; Zou, Z.-C.; Li, Q.-Y.; Nie, Z.-R. Large pore 3D cubic mesoporous silica HOM-5 for enzyme immobilization. *Mater. Lett.* **2008**, *62* (21−22), 3707−3709.
(33) Shang, C. Y.; Li, W. X.; Zhang, R. F. Immobilized *Candida antarctica* lipase B on ZnO nanowires/macroporous silica composites for catalyzing chiral resolution of (*R*,*S*)-2-octanol. *Enzyme Microb. Technol.* **2014**, *61*−*62*, 28−34.
(34) Sun, J.; Du, K.; Fu, L.; Gao, J.; Zhang, H.; Feng, W.; Ji, P. Sodium hexadecyl sulfate as an interfacial substance adjusting the adsorption of a protein on carbon nanotubes. *ACS Appl. Mater. Interfaces* **2014**, *6* (17), 15132−15139.
(35) Kao, K.-C.; Lin, T.-S.; Mou, C.-Y. Enhanced activity and stability of lysozyme by immobilization in the matching nanochannels of mesoporous silica nanoparticles. *J. Phys. Chem. C* **2014**, *118* (13), 6734−6743.
(36) Han, Z. P.; Fu, J.; Ye, P.; Dong, X. P. A general strategy for protein immobilization in layered titanates: Polyelectrolyte-assisted self-assembly. *Enzyme Microb. Technol.* **2013**, *53* (2), 79−84.
(37) Kubiak-Ossowska, K.; Mulheran, P. A. Mechanism of hen egg white lysozyme adsorption on a charged solid surface. *Langmuir* **2010**, *26* (20), 15954−15965.
(38) Li, L. L.; Wang, H. Enzyme-coated mesoporous silica nanoparticles as efficient antibacterial agents in vivo. *Adv. Healthcare Mater.* **2013**, *2* (10), 1351−1360.

DOI: 10.1021/acssuschemeng.5b00104
ACS Sustainable Chem. Eng. 2015, 3, 1183−1189